

Computational Modeling of Torpedo Anchor Penetration at Seabed Using Piezocone Tests

T. Almeida¹, C. Varady¹, J. Tenório¹, J. Santos², R. Dias³, and F. Cutrim³

¹*Laboratório de Computação Científica e Visualização, Universidade Federal de Alagoas
Cidade Universitária, Maceió, 57072-900, Alagoas, Brasil
tacio.almeida@ctec.ufal.br, christiano_varady@lccv.ufal.br, joyce.tenorio@lccv.ufal.br*

²*Centro de Tecnologia, Universidade Federal de Alagoas
Cidade Universitária, Maceió, 57072-900, Alagoas, Brasil
joao.santos@ctec.ufal.br*

³*Centro de Pesquisas, Desenvolvimento e Inovação Leopoldo Américo Miguez de Mello - CENPES/PETROBRAS
Avenida Horácio Macedo, 950, Cidade Universitária, Rio de Janeiro, 21941-915, Rio de Janeiro
rafael_dias@petrobras.com.br, fabiosawada@petrobras.com.br*

Abstract. The present work assesses the dynamics of torpedo anchor penetration at the seabed, leveraging real marine soil data obtained from Piezocone Tests (CPTu tests) provided by a Brazilian oil and gas company. The study brings new possibilities to methods proposed in previous works, such as True (1974), by improving its calculation model regarding the acting forces and the soil characterization. Implementing the controlled speed motion comes from the need to predict the embedment depth when using this type of penetration process. Also, the comparison between the free-fall and the controlled speed motion can be seen as an important feature in the context of torpedo anchor penetration. The utilization of CPTu tests allows a coherent and more complete characterization of the behavior of the undrained shear strength and the specific weight of cohesive soils since it provides a large amount of data that can satisfactorily describe the soil profile. So, the comparison between one-layer and multiple-layer solutions can be seen in terms of the accuracy of the results and computational cost. The improvement of the calculation model allows a better characterization of the heterogeneous soil profiles and the utilization of the fourth-order Runge-Kutta method provides better results in comparison to the existing process.

Keywords: Cravability, Torpedo Base, CPTu.

1 Introduction

The application of a torpedo base, characterized as a heavy ballast free-fall pile, reduces the anchoring installation cost and improves the short precision. The operator releases the torpedo from a certain height of the mudline. Upon the impact, the torpedo hits the soil with an initial speed value, reaching the embedment depth [1]. The installation can occur by a free-fall motion, when the pile is free to accelerate since no external agents are acting; or by controlled velocity motion, when the pile continues attached to the crane throughout the driving process and slows down as the friction forces increase.

While the pile penetrates the soil, friction forces decelerate the object until it reaches the final embedment depth. Evaluating the embedment depth based on soil and pile characteristics is crucial, as it serves as the foundation for the structure that will be placed on it. Previous works employed numerical methods to calculate the embedment depth of a torpedo anchor on marine clay with different densities and strength [2][3], and assessed the influence of the strain rate and strain softening on embedment depth of a torpedo anchor in clay [4]. Besides, for proper soil characterization, existing methods can be used to classify the soil layers and also simplify the problem [5].

For proper cravability analysis, it is important to address the undrained shear strength behavior in any soil, as it indicates the soil's capability to cease pile movement. This information can be calculated from Piezocone Tests (CPTu), which is a test used to determine soil characteristics by getting the soil resistance at the tip of the anchor and the friction along the lateral area of the penetrometer, along the soil profile [6]. So, this procedure provides the behavior of the undrained shear strength and the specific weight within a layer profile.

In this matter, the present work aims to predict the embedment depth of the torpedo anchor, using soil char-

acteristics based on CPTu tests. The present work uses True's numerical methodology [2], adapts it to multiple layers and different installation profiles (free-fall and controlled speed), and compares it in terms of embedment depth and friction forces behavior. However, considering the limitations of the used methodology, this work must be limited to cohesive soils, since the physical description of the problem may not be accurate for noncohesive soils, like sand.

2 Methodology

True (1974) analyzed the phenomenon of the torpedo anchor penetration into seafloor soils by free-fall. Applying Newton's Second Law, the penetration behavior consists of the buoyant weight (W_B) promoting the increase of the speed while the drag (F_H), the bearing (F_{BE}) and the side adhesion (F_{AD}) forces eventually overcoming and slowing down the anchor, as illustrated in Fig. 1. The sum of these forces is equal to the product between the mass m and the acceleration, as shows the following expression:

$$m \frac{dv}{dt} = W_B - (F_H + F_{BE} + F_{AD}). \quad (1)$$

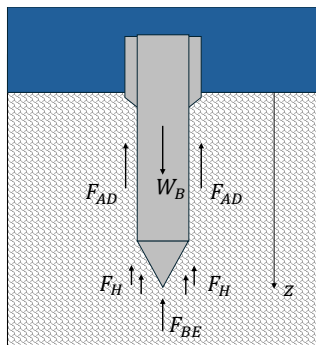


Figure 1. Forces on a penetrating object

First, the only force favorable to the movement is the pile weight, which is the sum of the object's weight (W) and the portions of buoyancy generated by the water (B_{water}) and the soil (B_{soil}), as shown in eq. (2):

$$W_B = W - (B_{water} + B_{soil}). \quad (2)$$

Thus, the drag force (F_H) caused by the friction between an object and the water or the soil, is determined by the product between the drag coefficient (C_D), the frontal torpedo's frontal area (A_F), the soil's specific weight (γ) and the square of the speed (v), divided by two times the gravity, which can be seen in eq. (3):

$$F_H = \frac{1}{2g} \gamma C_D A_F v^2. \quad (3)$$

Moreover, the bearing and the side adhesion forces are calculated using some soil parameters used by the author. The bearing force is equal to the product between the undrained shear strength at the tip of the anchor (S_u), the frontal area (A_F), the bearing capacity factor (N_C) and the division between the strain rate coefficient (S_e) and it's maximum value at high velocities (S_e^*), as shown in eq. (4). Meanwhile, the side adhesion force is equal to the product between the average undrained shear strength on the lateral area of the anchor ($\overline{S_u}$), the division between the side adhesion factor (δ) and the soil sensitivity (S_t) and again the division between S_e and S_e^* , as shown in eq. (5):

$$F_B = S_u A_F N_C \frac{S_e}{S_e^*}, \quad (4)$$

$$F_{AD} = \overline{S_u} \frac{\delta S_e}{S_t S_e^*} \quad (5)$$

Also, the inverse of S_e^* is calculated by the following expression, using parameters as the other strain rate coefficient (C_e), the speed (v), the undrained shear strength at the tip of the anchor (S_u), the anchor diameter (d) and an arbitrary constant value (C_0). The expression can be seen in eq. (6):

$$\frac{1}{S_e^*} = \frac{1}{1 + \frac{1}{\sqrt{\frac{C_e v}{S_u d} + C_0}}} \quad (6)$$

From the development of the multiple soil layer characterization, the calculation of the forces must account for the possibility of the penetration object passing through multiple soil layers. So the drag force, the side adhesion force and the buoyant weight are calculated as the sum of small portions, which are calculated in terms of the soil parameters of each layer containing the torpedo anchor. Also, the bearing force is calculated by taking the soil parameters of the layer that contains the tip of the anchor.

Table 1 shows the geometrical and physical characteristics of the torpedo anchor and 2 presents the soil parameters used in tests and found in the literature.

Table 1. Torpedo anchor characteristics

Buoyant weight (kN)	Length (m)	Diameter (m)	Specific weight (kN/m ³)
418.00	18.50	0.76	52.43

Table 2. Soil empiric parameters

δ	S_t	N_c	C_D	C_0	C_{e1} (kPas)	C_{e2} (kPas)	S_{e1}	S_{e2}
0.90	2.00	9.00	0.70	0.06	4.50	11.00	2.50	2.70

CPTu tests from Campos Basin were used to characterize the undrained shear strength and the specific weight for both one-layer and two-layer situations. Thus, the behaviour of the undrained shear strength and the specific weight are illustrated in Fig. 2. So the embedment depth calculated using the soil data, the one-layer and the two-layer situations can be compared in order to evaluate how much the problem can be simplified without a significant loss of accuracy in the process.

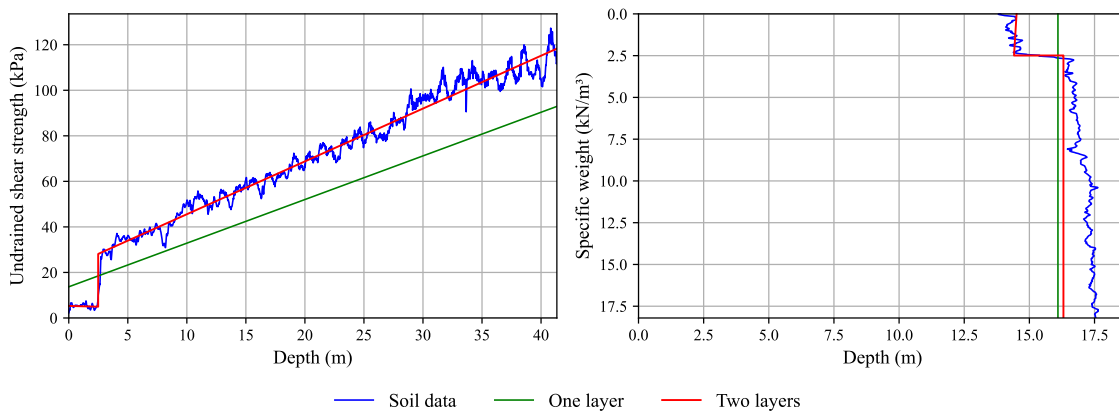


Figure 2. Multiple layer characterization

The values associated with the one-layer and the two-layer characterization are shown in Table 3. For each layer, the undrained shear strength will variate linearly with the depth and the specific weight will remain constant.

Table 3. Soil characterization

One layer characterization					
z_0 (m)	z_f (m)	S_{u0} (kPa)	S_{uf} (kPa)	γ_s (kN/m ³)	
0	41.4	9.6	65.0	16.1	
Two layers characterization					
z_0 (m)	z_f (m)	S_{u0} (kPa)	S_{uf} (kPa)	γ_s (kN/m ³)	
0	2.49	2.8	2.7	14.5	
2.49	41.4	15.2	63.9	16.3	

For the controlled speed model, the method is adapted to verify if the resulting force in the anchor is positive downwards. If so, there will be no increase in the speed, which makes it impossible for the object accelerates positively downwards. Also, from the moment that the resulting forces become zero and begins to be positive upwards, the speed control is ceased making the velocity decrease as the anchor penetrates and eventually turn to zero, meaning that it reached the final embedment depth value. Lastly, the general procedure is illustrated in Fig. 3, which shows the step-by-step scheme used for obtain the results. Also, Runge-Kutta and Euler method were used to solve the differential equation in order to evaluate the accuracy of both techniques.

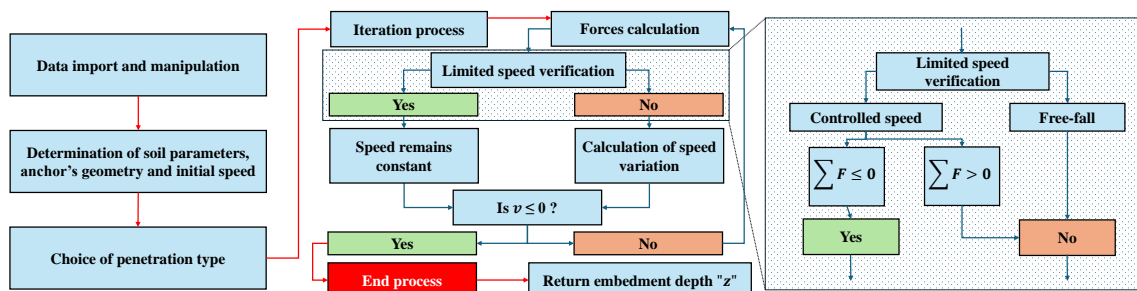


Figure 3. Cravability model flowchart

3 Results and Discussions

Embedment depth from different initial velocities was calculated using Euler’s and Runge-Kutta techniques for solving differential equations and are presented in Table 4. It is noted that the difference gets slightly higher at lower initial speed values, for both free-fall and controlled speed motion. However, in some controlled speed cases, Euler’s method diverged and the motion did not cease, which does not happen using the Runge-Kutta procedure.

Table 4. Embedment depth values

Initial speed (m/s)	0.67	1.33	2.00	4.00	6.00	8.00
Euler embedment depth (m)	9.3	9.7	9.9	10.6	11.6	12.8
Runge-Kutta embedment depth (m)	9.9	9.9	10.0	10.7	11.7	12.9

In terms of the speed profile, for a one-layered soil situation, when the speed is limited, the embedment depth tends to have lower values, as we can see in Fig. 4, which can be explained by the fact that, when the speed is not

controlled, the torpedo anchor can increase its momentum and reach deeper into the soil. As the initial speed is increased, the embedment depth values in both cases tend to converge, which may imply that for bigger velocities these values tend to be the same. This can be explained by the fact that some forces are greater as that speed increases, like the drag force.

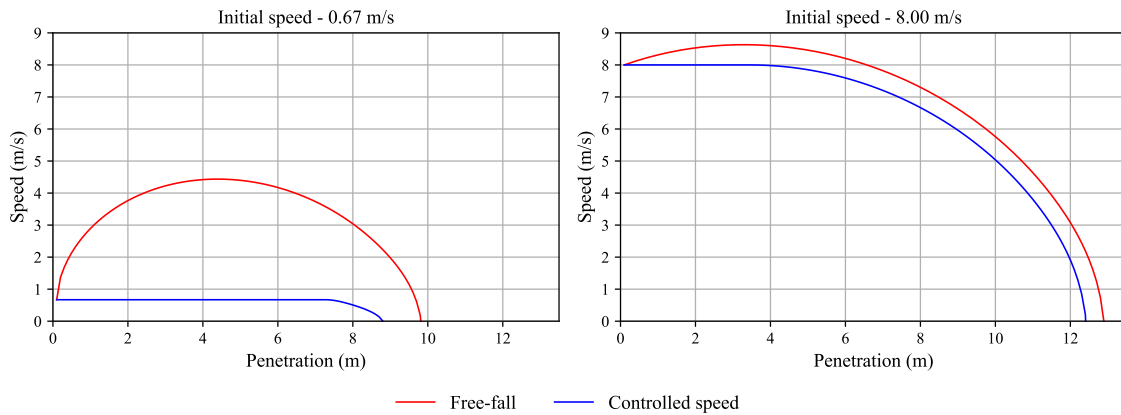


Figure 4. Variation of speed results

In this context, evaluating the variation of the acting forces, all the friction forces tend to reach lower values when the speed is limited when compared to the free-fall situation, but again this difference gets smaller the bigger the initial speed value. This reinforces the possibility that with greater speed values, the greater the friction forces values, as shown in Fig. 5, and theoretically there may be a minimum initial speed value in which the embedment depth will be the same for both situations.

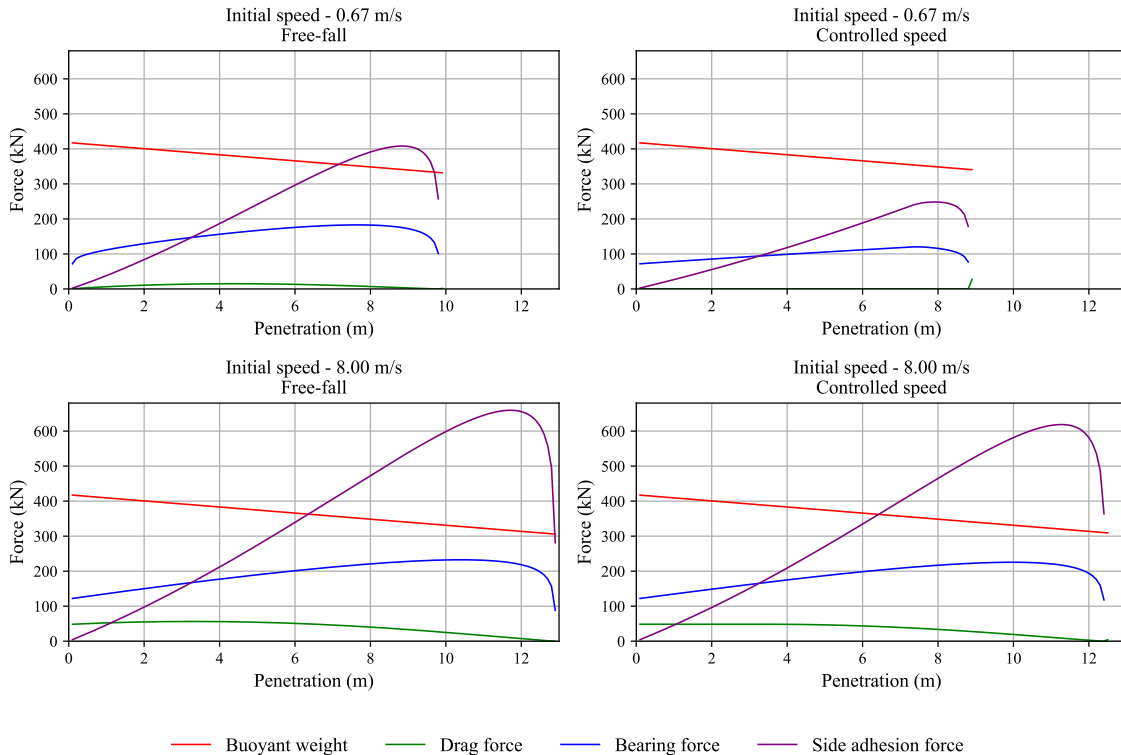


Figure 5. Variation of forces results for different scenarios

On the other hand, the multiple soil layers characterization brings a substantial difference in terms of the ac-

curacy of the results, especially when the cravation needs to be done in heterogeneous soil with deep penetrations. It is possible to see that, although the one-layer characterization can be relatively accurate when comparing relatively homogeneous soil layers. In this scenario, there was a significant difference between both characterizations, as illustrated in Fig. 6 which is bigger for smaller initial speed values, for free-fall and controlled speed.

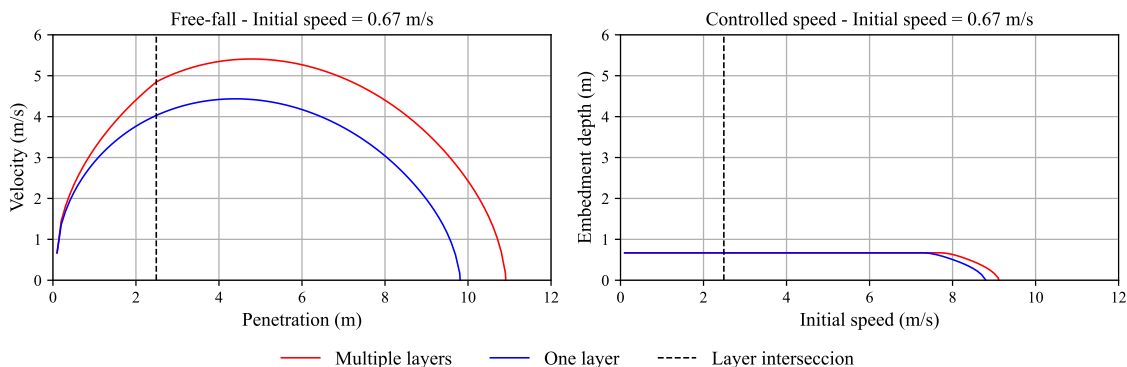


Figure 6. Speed variation comparison

Therefore, this difference can be seen in forces variation as well, where the difference in acceleration can be explained by how some forces behave in a situation of heterogeneous soil, as shown in Fig. 7. In fact, on the intersection between two layers of a heterogeneous soil, the bearing force and the side adhesion force show a discontinuance due to the behavior of the undrained shear strength.

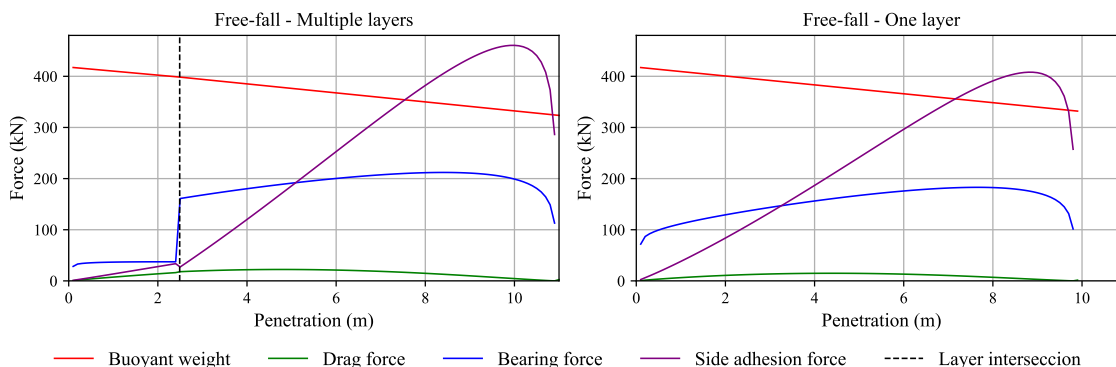


Figure 7. Force variation comparison

4 Conclusions

This study evaluated modifications to True’s methodology, proposing its broader application. In general, it was possible to see that the controlled speed motion and the multiple layers characterization showed coherent results and can be applied in this method. However, the empiric strain rate coefficients used at the controlled speed motion situations need to be calculated from similar situations.

First, the implementation of the Runge-Kutta method for solving differential equations was necessary to provide more accuracy. Although the Euler’s method showed similar results in most cases, for small initial speed values the Euler’s method may not be able to deliver a coherent result. The controlled speed penetration feature allowed the comparison between this case and the free-fall. For the studied cases, the free-fall embedment depth will be higher than the other case, however the difference gets smaller for increased initial speed value. Considering the multiple layers characterization, the simplification of the soil layers data can provide less computational cost but will deliver less accurate results, especially when the soil profile is not homogeneous.

Therefore, due to limitations brought with previous works, there is space for amplifying the number of scenarios by improving the physical characterization, especially in terms of undrained shear strength, strain rate, and strain softening behavior.

Acknowledgements. The authors would like to thank PETROBRAS for the financial support related to the development of this research project.

Authorship statement. The authors hereby confirm that they are the sole liable persons responsible for the authorship of this work, and that all material that has been herein included as part of the present paper is either the property (and authorship) of the authors, or has the permission of the owners to be included here.

References

- [1] C. F. Mastrangelo, P. J. Barusco, J. M. Formigli, and R. Dias. From early production systems to the development of ultra deepwater fields: experience and critical issues of floating production units. *Offshore Technology Conference*, vol. 1, n. 1, pp. 1–14, 2003.
- [2] D. G. True. Rapid penetration into seafloor soils. *Offshore Technology Conference*, vol. 1, n. 2095, pp. 1–12, 1974.
- [3] D. G. True. Rapid penetration into seafloor soils. *Journal of Hydronautics*, vol. 9, n. 1, pp. 69–77, 1975.
- [4] Y. Kim, M. Hossain, and D. Wang. Effect of strain rate and strain softening on embedment depth of a torpedo anchor in clay. *Ocean Engineering*, vol. 108, n. 1, pp. 704–715, 2015.
- [5] P. K. Robertson. Soil classification using the cone penetration test. *Canadian Geotechnical Journal*, vol. 27, n. 2, pp. 151–158, 1990.
- [6] T. Lunne, J. J. M. Powell, and P. K. Robertson. *Cone Penetration Testing in Geotechnical Practice*. CRC Press, 1997.